Model-space nuclear matter calculations with the Paris nucleon-nucleon potential

T. T. S. Kuo, Z. Y. Ma,* and R. Vinh Mau†
Department of Physics, State University of New York at Stony Brook, Stony Brook, New York 11794
(Received 2 August 1985)

Using a model-space Brueckner-Hartree-Fock approach, we have carried out nuclear matter calculations using the Paris nucleon-nucleon potential. The self-consistent single particle spectrum from this approach is continuous for momentum up to k_M, where $k_M \approx 2k_F$ is the momentum space boundary of our chosen model space. The nuclear matter average binding energy and saturation Fermi momentum given by our calculations are ~ 15.6 MeV and ~ 1.56 fm^{-1}, respectively. When using the conventional Brueckner-Hartree-Fock approach with a spectrum which has a gap at k_F, the corresponding results are ~ 11.5 MeV and ~ 1.50 fm^{-1}. The gain of approximately 4 MeV in binding energy between the two calculations comes mainly from the $^3S_1$ and $^1S_0$ partial wave channels. We have investigated the effect of adding an empirical density dependent central potential to the Paris potential. It is found that the addition of such a potential whose strength is $\sim 10\%$ of the central component of the Paris potential is adequate in making the nuclear matter binding energy and saturation density in simultaneous agreement with the empirical values.

I. INTRODUCTION

In recent years nucleon-nucleon potentials derived from meson and isobar degrees of freedom have been able to describe rather satisfactorily experimental nucleon-nucleon phase shifts and deuteron properties. The next question to be answered is whether such potentials are able to predict nuclear many-body properties. As is well known, the simplest many-body system as far as theoretical calculations are concerned is the infinitely large and homogeneous nuclear matter. Many methods have been proposed for carrying out nuclear matter calculations, such as the Brueckner-Hartree-Fock (BHF),[1] the Fermi hypernetted chain,[2] the e^S (Ref. 3), and the model-space BHF (Refs. 4 and 5) methods. From the Weiszäcker empirical nuclear mass formula, the binding energy per nucleon (BE/A) in nuclear matter is deduced to be ~ 16 MeV, and from electron scattering experiments of nuclei, the nuclear matter saturation density (ρ_0) is deduced to be ~ 0.17 nucleon per fm^3. Theoretical derivations using the methods mentioned above have, however, never been able to reproduce the values of the binding energy per nucleon (BE/A) and ρ_0 which are in simultaneous agreement with the corresponding empirical values; the calculated values of BE/A and ρ_0 using various nucleon-nucleon potentials generally lie on a band—the Coester band[6]—which deviates significantly from the corresponding empirical values. This deviation can be attributed to different sources. It could be due to the inadequacy of the many-body techniques used so far in the calculations. It could also be that the assumption that two-body forces are dominant in nuclear matter is not accurate enough and that three or more body forces are not negligible. This point was, in fact, suggested by several recent studies,[8,9] although, even in the case of three-body forces, the derivation of these forces is still very ambiguous.

In this paper, we report our results of several model-space BHF (MBHF) calculations of nuclear matter, using the Paris nucleon-nucleon (NN) potential.[7] This method was introduced by Ma and Kuo.[4] They have applied it using the Reid NN potential. They have also carried out some preliminary MBHF nuclear matter calculations using the Paris NN potential, including only partial waves with $l \leq 5$. Results of these calculations have been very briefly reported.[5] The present paper carries out more extensive MBHF calculations using the Paris NN potential and will report the results in more detail. In addition, we will study the effect of adding an empirical density dependent two-body effective interaction to the Paris potential. This effective density dependent interaction is assumed to represent all effects due to the modification of the two-body forces by the medium, three-body forces, etc. We will show indeed that we only need to add a fairly small density dependent component to the Paris potential so as to make the calculated nuclear matter saturation density in good agreement with the experimental one.

We will first, in Sec. II, briefly describe the MBHF method for nuclear matter calculations. Mahaux and his collaborators[10] have pointed out that the discontinuous single particle spectrum used in conventional BHF calculations is unsatisfactory on several fundamental grounds, mainly because this spectrum has an artificial energy gap of ~ 60 MeV at the Fermi surface k_F. These authors therefore proposed a continuous single particle spectrum based on a Green's function method. The MBHF method is derived from a model-space approach, which leads to a single particle spectrum which is continuous within the chosen model space. Hence if one chooses a model space which extends beyond k_F, one will obtain a single particle spectrum which is continuous is k_F. As discussed later, one may choose to treat the hole-line spectrum slightly different when carrying out nuclear matter calculations within the model space. Then the resulting single particle spectrum will have a small gap at k_F. An important feature of our spectrum is that its potential energy is generally attractive in the momentum region k_F to $\sim 2k_F$. In

Sec. III we will report on our results of nuclear matter calculations by using the Paris nucleon-nucleon potential as well as describing some details of our computational methods, such as the Born approximation for calculating the potential energy contribution from partial waves with $l \geq 5$. In Sec. IV, we will describe and discuss several MBHF nuclear matter calculations using the Paris nucleon-nucleon potential with its central component modified by an empirical density dependent factor. A discussion and a conclusion are presented in Sec. V.

II. THE MBHF METHOD FOR NUCLEAR MATTER

In this section we briefly describe the MBHF method for nuclear matter.[4,5] In treating nuclear many-body problems, one usually introduces a one-body auxiliary potential U to the nuclear Hamiltonian $H=T+V$, where V is a chosen nucleon-nucleon (NN) potential, and rewrite it as

$$H=(T+U)+(V-U)\equiv H_0+H_1 \ . \tag{1}$$

The exact solutions of the Schrödinger equation

$$H\psi_n=E_n\psi_n \tag{2}$$

are, of course, independent of the choice of U. But when solving Eq. (2), using some approximation methods as invariably done in practice, the choice of U can play a very important role. The MBHF method is basically a method for the choice of U. For nuclear matter calculations, we begin with choosing a model space P defined by

$$P\equiv\{k\leq k_M\} \ , \tag{3}$$

where all nucleons are restricted to have momentum k less than k_M, the momentum space boundary of P. Typical values for k_M are ~ 3 fm^{-1}, as will be discussed later. Using effective interaction theories,[11,12] we can transform Eq. (2) into a model space equation

$$H_{\rm eff}P\psi_m=E_mP\psi_m \ , \tag{4}$$

with

$$H_{\rm eff}=P(H_0+V_{\rm eff})P \ , \tag{4a}$$

where $H_{\rm eff}$ and $V_{\rm eff}$ are, respectively, the model-space effective Hamiltonian and interaction. Clearly $V_{\rm eff}$ itself is dependent on U.

The effective interaction $V_{\rm eff}$ generally contains many-body components, i.e.,

$$V_{\rm eff}=\bar{V}^{(0)}+\bar{V}^{(1)}+\bar{V}^{(2)}+\cdots \ , \tag{5}$$

where $\bar{V}^{(n)}$ denotes the n-body components of $V_{\rm eff}$. This is so even when the original interaction V is taken merely as a two-body interaction, such as the Paris potential.[17] A basic step of the MBHF method is to choose U such that

$$P\bar{V}^{(1)}P=0 \ . \tag{6}$$

This is in fact a model-space Hartree-Fock condition, as it is equivalent to requiring $\langle 1p1h \mid PH_{\rm eff}P \mid 0p0h\rangle=0$ where 1p1h and 0p0h are the familiar one-particle–one-hole and zero-particle–zero-hole eigenstates of H_0, respectively. From Eq. (6) we can only determine PUP, and we have chosen $PUQ=QUP=QUQ=0$.[4,5] Let us mention that the unknown to be solved for from Eq. (6) is PUP, and in doing so a self-consistent procedure must be employed. This is because, briefly speaking, we need to know H_0 and P in order to calculate the matrix elements of U from Eq. (6), while H_0 and P themselves are also dependent on U. For nuclear matter, this self-consistent procedure is simplified because our P, given in terms of plane-wave single particle states, is independent of U. As in Ref. 4, we use a one-G-matrix approximation in solving Eq. (6), and this leads to the following self-consistent equations for PUP:

$$\langle k \mid U^{\rm MHF} \mid k\rangle=\sum_{h\leq k_F}\langle kh \mid \bar{G}(\omega) \mid kh\rangle \ , \tag{7}$$

$$\langle kh \mid \bar{G}(\omega) \mid kh\rangle = \langle kh \mid V \mid kh\rangle + \sum_{mn}\frac{\langle kh \mid V \mid mn\rangle\bar{Q}(mn)\langle mn \mid \bar{G}(\omega) \mid kh\rangle}{\omega-\epsilon_n^M-\epsilon_m^M} \ , \tag{7a}$$

$$\omega=\epsilon_k^M+\epsilon_h^M \ , \tag{7b}$$

$$\epsilon_l^M=t_l+\langle k_l \mid u^{\rm MHF} \mid k_l\rangle, \quad k_l\leq k_M \ , \qquad =t_l, \quad k_l>k_M \ , \tag{7c}$$

where t_l is the kinetic energy $\hbar^2k_l^2/2m$. U and $U^{\rm MHF}$ are related by $U=\sum_{i=1}^{A}u^{\rm MHF}(i)$. Note that the intermediate states of the $\bar{G}$ matrix must belong to the Q space, and this is ensured by using in Eq. (7a)

$$\bar{Q}(mn)=1, \text{ if } \max(k_m,k_n)>k_M \text{ and } \min(k_m,k_n)>k_F \ , \qquad =0, \text{ otherwise} \ . \tag{7d}$$

An angle-average approximation for $\bar{Q}$ (Ref. 4) has been used in our calculations. In this way, $\bar{Q}$ is dependent only on the magnitudes of the center of mass and relative momenta $\mathbf{K}$ and $\mathbf{k}$. Then, as shown in Fig. 1, the values of $\bar{Q}$ are calculated depending on which regions the magnitudes of K and k belong to. These regions (a to f) are di-

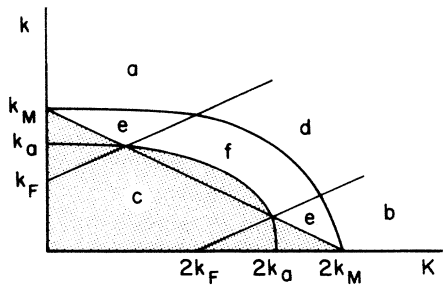

FIG. 1. Angle averaged projection operator $\bar{Q}(m,n)$ of Eq. (7). k_a^2 is $(k_F^2+k_M^2)/2$.

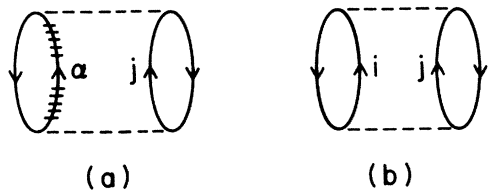

FIG. 2. Structure of $\overline{G}$ and G_M matrices. Particles with momentum $>k_M$ are denoted by railed lines. Bare particle lines are those with momentum $\leq k_M$.

vided by three lines, $k-K/2=\pm k_F$ and $k+K/2=k_M$, and two ellipses $k^2+K^2/4=k_M^2$ and $(k_F^2+k_M^2)/2$. In regions a and b we have $\overline{Q}=1$, and in the shaded region c we have $\overline{Q}=0$. The angle-averaged approximations are used only for regions d, e, and f, and the values of $\overline{Q}$ in these regions are, respectively, $(k^2-k_F^2-K^2/4)/kK$, $[(k+K/2)^2-k_M^2]/kK$, and $(2k^2-k_F^2-k_M^2+K^2/2)/kK$.

The $\overline{G}$ interaction defined above contains only those diagrams whose intermediate states have at least one particle with momentum $>k_M$. In nuclear matter calculations, particle-hole excitations with particle momentum $<k_M$ should also be included, and this can be done by including processes corresponding to repeated $\overline{G}$ interactions within the model space P. Let us give some examples. As shown in Fig. 2, diagram (a) is contained in $\overline{G}$ but not (b). This is because the bare particle lines i and j both have momentum $<k_M$, while the railed line α is a line with momentum $>k_M$. To include diagram (b) in the nuclear matter calculation, we need to calculate diagrams second order in $\overline{G}$. To include this type of diagram more completely, we adopt the MBHF method.[4] Briefly speaking, we first calculate the model-space two-body effective interaction by including $\overline{G}$ and all the two-body folded diagrams generated by $\overline{G}$, i.e.,

$$V_{\text{eff}}^{(2)}\approx\overline{G}-\overline{G}\int\overline{G}+\overline{G}\int\overline{G}\int\overline{G}-\cdots\equiv\overline{G}_F\ . \tag{8}$$

We then carry out BHF nuclear matter calculations within the model space, using the $\overline{G}_F$ as the effective nucleon-nucleon interaction within the model space. This leads to the following self-consistent equations:

$$\langle h_1h_2\,|\,G_M(\omega)\,|\,h_1h_2\rangle=\langle h_1h_2\,|\,\overline{G}_F\,|\,h_1h_2\rangle+\sum_{mn}\frac{\langle h_1h_2\,|\,\overline{G}_F\,|\,mn\rangle Q(mn)\langle mn\,|\,G_M(\omega)\,|\,h_1h_2\rangle}{\omega-\epsilon_m-\epsilon_n}\ , \tag{9}$$

where $\omega=\epsilon_{h_1}+\epsilon_{h_2}$ and

$$Q(m,n)=1,\ \text{if}\ k_F<(k_m,k_n)\leq k_M\ ,$$
$$=0,\ \text{otherwise}\ , \tag{9a}$$

$$\epsilon_m=t_m+\sum_{h<k_F}\langle mh\,|\,G_M(\epsilon_m+\epsilon_h)\,|\,mh\rangle\ \text{if}\ k_m\leq k_F\ ,$$
$$=\epsilon_m^M\ \text{if}\ k_m>k_F\ , \tag{9b}$$

where ϵ_m^M was given in Eq. (7b). The potential energy (PE) per particle in nuclear matter is given in terms of G_M by

$$\langle\text{PE}\rangle=\frac{1}{A}\sum_{h_1,h_2\leq k_F}\langle h_1h_2\,|\,G_M(\epsilon_{h_1}+\epsilon_{h_2})\,|\,h_1h_2\rangle \tag{9c}$$

with the single particle energies ϵ given by Eq. (9b).

We can simplify the above calculations. By substituting $\overline{G}_F$ of Eq. (8) into Eq. (9) and making use of Eqs. (7a)–(7d), we can rewrite Eq. (9) as

$$\langle h_1h_2\,|\,G_M(\omega)\,|\,h_1h_2\rangle=\langle h_1h_2\,|\,V\,|\,h_1h_2\rangle+\sum_{mn}\frac{\langle h_1h_2\,|\,V\,|\,mn\rangle[Q(mn)+\overline{Q}(mn)]\langle mn\,|\,G_M(\omega)\,|\,h_1h_2\rangle}{\omega-\epsilon_m-\epsilon_n} \tag{10}$$

with $\omega=\epsilon_{h_1}+\epsilon_{h_2}$ and Q and $\overline{Q}$ given, respectively, by Eqs. (7d) and (9a). Equation (10) is more convenient for calculation than Eq. (9), because we now calculate G_M directly from V whereas for Eq. (9) we need to first calculate $\overline{G}_F$ and then calculate G_M from $\overline{G}_F$. From Eq. (10) we can see rather clearly the connection between the MBHF method and the conventional BHF method. The essential difference is in the treatment of the single particle spectrum for $k>k_F$. In the BHF method, free-particle spectrum is used for particles with $k>k_F$. In the present method, free particle spectrum is used only for $k>k_M$, whereas the model-space HF spectrum of Eq. (7c) is used for $k_F<k<k_M$. It is easily seen that the above MBHF method reduces to the conventional BHF method if we choose $k_M=k_F$. How should we choose k_M? If the calculations are carried out exactly, the results should be independent of k_M. In practice, we must make some approximations, and therefore the choice of k_M will affect our results. We have found that for $k_M\sim 2k_F$ or ~ 3 fm^{-1} the results of our nuclear matter binding energy calculations are quite stable with respect to small variations of k_M.[5] We have therefore chosen $k_M=2k_F$ in our calculations.

III. NUCLEAR MATTER CALCULATIONS USING PARIS POTENTIAL

The Paris potential reproduces the low-energy ($E\lesssim 330$ MeV) two-nucleon scattering data and deuteron properties

very well, and its long- and medium-range parts are field theoretically derived including components from one-, two-, and three-pion exchanges. The short-range ($r<0.8$ fm) part of this potential is determined phenomenologically. In our nuclear matter calculations, we have used the parametrized form of this potential as the NN potential V of Eq. (1). This form of the Paris NN potential has a significant momentum dependent component which has been shown[13] to have important effects on the nuclear matter single-particle spectrum, effective mass, and binding energy. It should be pointed out that in numerical calculations special care must be given to the treatment of this momentum dependent component, as was found in coordinate space phase-shift and nuclear matter calculations.[13] We calculate the nuclear matter G matrix using momentum space integral equation methods, and have found that it is very important to treat the momentum space mesh points at high momentum (~ 30 fm^{-1}) with great care. A fairly high concentration of momentum space Gaussian points must be placed in this region in order to obtain numerical stability.

A first step in our calculation is the evaluation of the partial wave matrix element of the form

$$\langle kl \mid V \mid k'l' \rangle = \int_0^\infty r^2 dr\, j_l(kr) V(r) j_{l'}(k'r) , \tag{11}$$

where $V(r)$ is the Paris potential. This matrix element may be evaluated using numerical integration, but in this way high accuracy is difficult to obtain; this is because of the strong short-range components contained in $V(r)$ and the rapid oscillations of the Bessel functions when k and/or k' become large. The parametrized form of $V(r)$ is particularly convenient because it is composed of a sum of Yukawa terms of the form e^{-mr}/r and their derivatives. Then the matrix elements of Eq. (11) can be analytically evaluated by way of the integration formula

$$\int_0^\infty r^2 dr\, j_l(kr) \frac{e^{-mr}}{r} j_l(k'r) dr' = \frac{1}{2kk'} Q_l(z) , \tag{12}$$

where $z=(k^2+k'^2+m^2)/2kk'$ and $Q_l(z)$ is the Legendre function of the second kind. Thus the matrix elements $\langle kl \mid V \mid k'l' \rangle$ can be calculated either numerically or analytically. We have used both methods, and obtained satisfactory agreement between their results; this serves to check our computer programs. Results reported in this work were all carried out using analytically calculated $\langle kl \mid V \mid k'l' \rangle$.

The G_M matrix of Eq. (10) is then calculated in a partial wave basis, using angle average approximations for Q and $\bar{Q}$, namely

$$\langle k\alpha \mid G_M(\omega) \mid k'\alpha' \rangle = \langle k\alpha \mid V \mid k'\alpha' \rangle + \frac{2}{\pi} \int_0^\infty p^2 dp \sum_\beta \frac{\langle k\alpha \mid V \mid p\beta \rangle (Q+\bar{Q}) \langle p\beta \mid G_M(\omega) \mid k'\alpha' \rangle}{\omega - \epsilon_{k_1'} - \epsilon_{k_2'}} , \tag{13}$$

where α and β denote the two-nucleon partial wave quantum numbers ($lSTj$), k and k' the relative momenta, and $\epsilon_{k_1'}$ and $\epsilon_{k_2'}$ are the single particle energies given by Eq. (9b). The average potential energy per nucleon as given by Eq. (9c) is also calculated in terms of the partial wave G_M matrices, namely

$$\langle \mathrm{PE} \rangle = \sum_{k_1, k_2 \le k_F} \frac{4\pi}{A\Omega} \sum_\alpha (2T+1)(2j+1) \times \langle k\alpha \mid G_M(K^2) \mid k\alpha \rangle , \tag{14}$$

where A and Ω are, respectively, the mass number and volume of nuclear matter. The relative and center-of-mass momenta k and K are integrated over under the constraint that k_1 and k_2 are both less than k_F. ($\mathbf{k}_1=\mathbf{k}+\mathbf{K}/2$, $\mathbf{k}_2=\mathbf{k}-\mathbf{K}/2$.) Furthermore, an angle average approximation[1] for K^2 has been used in our calculation. For high partial waves ($l \ge 5$), short-range correlations between nucleons in nuclear matter are not important. Hence for these partial waves we have replaced G_M by V in Eq. (14). As shown in Table I, this replacement is judged to be a very accurate approximation for evaluating the nuclear matter potential energy for partial waves with $l \ge 4$. Here we see that the short-range correlations are important only for $l \le 2$ partial waves. For example, the $l=0$ contributions to U from V are generally repulsive. The main effect of including the short-range correlations is the conversion of V into G_M, and we see that the contributions from G_M are mostly attractive.

TABLE I. Average nuclear matter potential energies, in MeV, for various l values. The entries headed by G_M are calculated according to Eq. (14), while those under V are calculated in the same way except that G_M is replaced by V.

k_F (fm^{-1})	1.2		1.4		1.6	
l	V	G_M	V	G_M	V	G_M
0	29.97	−29.44	50.16	−37.66	77.99	−44.91
1	5.19	2.26	9.27	4.04	15.49	7.00
2	−2.91	−3.24	−5.56	−6.16	−9.54	−10.57
3	0.87	0.86	1.64	1.61	2.71	2.64
4	−0.48	−0.48	−1.09	−1.08	−2.12	−2.10

We have found that the high ($l>5$) partial waves have the effect of reducing the saturation density of nuclear matter. Their contribution to U at saturation density is found to be ~ 0.6 MeV per nucleon. In a previous calculation,[5] the $l>5$ partial waves were not included and the resulting saturation density was slightly larger than the one found in this work.

In Fig. 3, we show our results for the nuclear matter saturation curves, using the MBHF method as described above [mainly Eqs. (10), (13), and (14)] and elsewhere.[4,5] The average binding energy and saturation density are found to be 15.6 MeV and $k_F=1.56$ fm^{-1}, respectively. (The calculations were performed using $k_M=2k_F$.) We have also performed the usual BHF calculations, which correspond to the MBHF calculations with the special choice of $k_M=k_F$. As shown, saturation k_F and average binding energy for BHF are 1.5 fm^{-1} and 11.5 MeV, respectively. When compared with BHF, our MBHF calculations give an additional binding energy of ~ 4 MeV per nucleon. The nuclear matter incompressibility coefficient

$$\kappa=9\rho^2\frac{d^2}{d\rho^2}\left[\frac{E}{A}\right]_{k_F}=k^2\frac{d^2}{dk^2}\left[\frac{E}{A}\right]_{k_F} \tag{15}$$

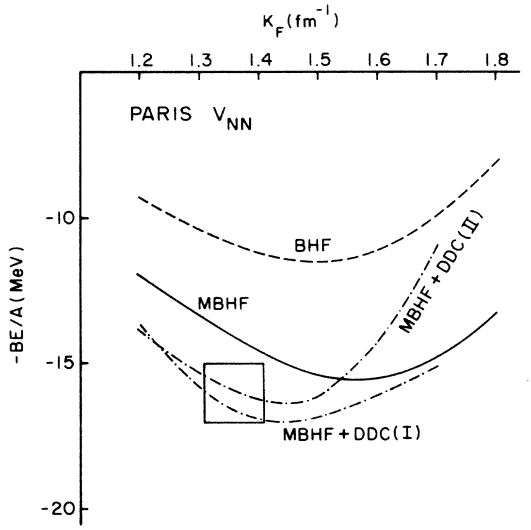

FIG. 3. Nuclear matter saturation curves. Curves BHF and MBHF are calculated using the Paris NN potential. The other two curves are both MBHF calculations using the Paris potential supplemented by density dependent central components. The binding energy per nucleon BE/A, saturation k_F and incompressibility coefficient κ for these curves are

Curve	BE/A	k_F	κ
BHF	11.5	1.50	153
MBHF	15.5	1.56	188
DDC(I)	17.1	1.45	231
DDC(II)	16.4	1.45	336

The empirical values for BE/A and saturation density are indicated by the box.

can be deduced from the saturation curves of Fig. 3. It is deduced to be approximately 150 MeV for BHF and 190 MeV for MBHF. Both are somewhat smaller than the empirical value of $\kappa=220\pm 20$ MeV.

In Table II, contributions to average potential energies from individual partial waves are tabulated, for two k_F values for both BHF and MBHF. As shown, the increase in binding energy from BHF to MBHF mainly comes from the $^3S_1$-$^3D_1$ and $^1S_0$ channels. (We have checked our computer programs by comparing our BHF results with those of Day.[14] For example, our BHF binding energy per nucleon at $k_F=1.4$ fm^{-1} is 11.19 MeV while his value is 11.15 MeV. In general, satisfactory agreement between our results and those of Day has been obtained.) As discussed in Sec. II and elsewhere,[4,5] an essential difference between BHF and MBHF is the choice or determination of the single particle spectrum ϵ_k used in nuclear matter calculations. Let us divide ϵ_k into three regions and express it as

$$\begin{aligned}\epsilon_k&=\frac{\hbar^2k^2}{2m_2^*}-\Delta_2 \quad \text{for } k<k_F\ ,\\ &=\frac{\hbar^2k^2}{2m_1^*}-\Delta_1 \quad \text{for } k_F<k<k_M\ ,\\ &=\frac{\hbar^2k^2}{2m} \quad \text{for } k>k_M\ .\end{aligned} \tag{16}$$

TABLE II. Decomposition of average nuclear matter potential energies (PE), in MeV, calculated from the Paris NN potential. See the text for other explanations.

k_F	1.4 (fm^{-1})		1.5 (fm^{-1})	
Channel	BHF	MBHF	BHF	MBHF
$^1S_0$	−16.97	−17.26	−19.16	−19.57
$^3S_1$-$^3S_1$	−17.99	−20.40	−19.29	−21.96
$^3D_1$-$^3D_1$	1.69	1.68	2.22	2.21
$^1P_1$	4.87	4.81	6.14	6.05
$^3P_0$	−3.84	−3.86	−4.52	−4.57
$^3P_1$	11.96	11.46	15.03	14.72
$^3P_2$-$^3P_2$	−8.14	−8.35	−10.65	−10.90
$^3F_2$-$^3F_2$	−0.69	−0.69	−0.95	−0.95
$^1D_2$	−3.21	−3.22	−4.30	−4.31
$^3D_2$	−4.65	−4.70	−6.13	−6.18
$^3D_3$-$^3D_3$	0.13	0.07	0.18	0.11
$^3G_3$-$^3G_3$	0.25	0.25	0.36	0.36
$^1F_3$	0.97	0.97	1.31	1.30
$^3F_3$	1.84	1.84	2.50	2.50
$^3F_4$-$^3F_4$	−0.51	−0.51	−0.76	−0.76
$^3H_4$-$^3H_4$	−0.11	−0.11	−0.17	−0.17
$^1G_4$	−0.56	−0.56	−0.79	−0.79
$^3G_4$	−0.87	−0.86	−1.24	−1.24
$^3G_5$-$^3G_5$	0.09	0.08	0.13	0.13
$^3I_5$-$^3I_5$	0.04	0.04	0.07	0.07
$l>4$	0.31	0.31	0.43	0.43
PE	−35.57	−38.94	−39.48	−43.41
KE	24.38	24.38	27.99	27.99
E/A	−11.19	−14.55	−11.49	−15.42

TABLE III. Single particle spectra derived from BHF and MBHF, using the Paris NN potential.

	1.4		1.5	
k_F	BHF	MBHF	BHF	MBHF
m/m_1^*	1	1.28	1	1.31
Δ_1	0	66.74	0	74.40
m/m_2^*	1.52	1.49	1.56	1.53
Δ_2	83.79	89.87	94.58	101.77

In MBHF, one first determines m_1^* and Δ_1 based on Eqs. (7). Then within the model space ($k<k_M$) we can further include the hole-line self-energy insertions. This leads to the (m_2^*,Δ_2) spectrum for $k<k_F$, as shown in Eq. (16). For $k>k_M$ we use the free particle spectrum. In Table III, we give some typical values for m_1^*, Δ_1, m_2^*, and Δ_2. In BHF, the self-consistent spectrum is used only for $k<k_F$, while the free particle is used for all other momenta. The values of m_2^* and Δ_2 for BHF are also shown in Table III. Clearly the MBHF and BHF spectrum are quite different for $k_F<k<k_M$. For $k<k_F$, the two are rather similar except that the MBHF spectrum is about 5 MeV lower than the BHF spectrum.

IV. DENSITY DEPENDENT CENTRAL POTENTIAL

We have seen that the binding energy per nucleon given by the MBHF nuclear matter calculations using the Paris NN potential is rather close to the empirical value of ~ 16 MeV/A. The saturation density given by such calculations is, however, larger than the empirical value corresponding to $k_F \sim 1.36$ fm^{-1}. Day[15] has pointed out that by using only a two-body NN interaction that fits the low energy scattering data and the deuteron properties, it is difficult to reproduce the empirical nuclear matter saturation properties. One can therefore conjecture that a density dependent component in the bare NN interaction for nucleons in nuclear matter may be needed. Based on our calculations, we would like this component to have a net repulsive effect in nuclear matter binding energy calculations for $k_F \gtrsim 1.5$ fm^{-1}, while for $k_F \lesssim 1.5$ fm^{-1} it should have a net attractive effect. Recently there has been much discussion on the effect of the three-body NN interaction in nuclear matter calculations. Although the effect of three-body and higher-body NN interactions to nuclear matter binding energy calculations may be small as compared to the contribution from the two-body NN interaction, their effect on nuclear matter saturation properties may, however, not be negligible.

In this work, we would like to investigate the effect of an empirical density dependent force in nuclear matter saturation density calculations. Our purpose is mainly to estimate the general strength of such a density dependent force so that its addition to the Paris NN potential will shift the nuclear matter saturation density given by MBHF to $k_F \approx 1.36$ fm^{-1}. We regard this density dependent central (DDC) piece as an empirical device to account for effects other than the two-body forces. It is well-known that a three-body force in nuclear matter can be generally represented by a two-body density dependent force. Thus we introduce a parametrized density dependent two-body force

$$V_{\rm DDC}(k_F)=\alpha e^{-\beta(k_F-k_0)^2}V_C$$

where V_C is the isospin independent central component of the Paris NN potential. α, β, and k_0 are parameters. We have performed MBHF calculations using various values for α, β, and k_0. In Fig. 3, the curve labeled MBHF + DDC(I) is obtained using $\alpha=0.1$, $\beta=20$ fm^2, and $k_0=1.30$ fm^{-1}. The NN interaction used in this MBHF calculation is given by the sum of $V_{\rm Paris}$ and $V_{\rm DDC}$. As shown, the resulting saturation Fermi momentum and binding energy per nucleon are, respectively, ~ 1.45 fm^{-1} and ~ 17 MeV, in good agreement with the empirical values. The resulting incompressibility coefficient is ~ 230 MeV, which is also in good agreement with the empirical value of $\sim 200\pm 20$ MeV. The above results indicate clearly that we only need a rather weak density-dependent two-body central interaction, whose strength is of the order of 10% of that of the Paris central potential, in order to bring the calculated nuclear matter saturation density and binding energy in simultaneous agreement with the empirical values. Based on a σ model, Jackson, Rho, and Krotscheck[9] have investigated the three-body forces for nucleons in nuclear matter. They suggested that the main effect of such forces may be represented by a two-body effective central interaction due to one σ-meson exchange with effective mass m'_σ, which is related to the bare mass m_σ by $m'_\sigma \approx m_\sigma\,(1-\alpha\rho+\beta\rho^{5/3})$, where ρ is the nuclear matter density. The constants α and β were given as ~ 0.5 fm^3 and ~ 1.2 fm^5, respectively. The medium range attraction of the NN potential comes mainly from the σ exchange. Thus, the renormalized m'_σ makes this part of the NN interaction density dependent. It is difficult to rigorously incorporate this effect into the Paris NN potential, because its medium range attractive part is due to the $\pi\pi$ S wave interaction rather than a "σ meson." As a preliminary investigation, we have simply modified the central part of the Paris potential V_C by a similar density dependent factor, converting it into $V_C/(1-\alpha'\rho+\beta'\rho^{5/3})$. When using this modified potential with $\alpha'=1.7$ fm^3 and $\beta'=4.3$ fm^5 in our MBHF calculation of nuclear matter, the resulting binding energy and saturation density are both in reasonably good agreement with the empirical values, as shown by the curve MBHF + DDC(II) of Fig. 3. The incompressibility coefficient obtained from this curve is ~ 336 MeV, which is somewhat too large as compared with the empirical value.

V. DISCUSSION AND CONCLUSION

We have carried out MBHF nuclear matter calculations using the Paris NN potential. Comparing with the corresponding BHF results, MBHF gives an additional binding energy of about 4 MeV per nucleon while slightly increasing the saturation density. The trend of these results is approximately the same as that observed in a MBHF calculation of nuclear matter using the Reid NN potential.[4,5]

The main difference between MBHF and BHF is the use of the single particle potential. Using a model-space HF approach, the self-consistent single particle spectrum given by MBHF is a continuous one for momentum $0<k<k_M$ where k_M is the chosen momentum-space model-space boundary. If one chooses $k_M>k_F$, then one has a continuous single particle spectrum extended beyond k_F. If one chooses $k_M=k_F$, then MBHF reduces to BHF whose single particle spectrum has a huge discontinuity at k_F; this is rather unphysical, as has been pointed by Mahaux and his collaborators[10,13] some time ago. Nuclear matter calculations are numerically rather complicated, and it will be very helpful to have checks with independent calculations. The present calculation is rather similar to a recent nuclear matter calculation using the Paris NN potential carried out by Lejeune, Martzolff, and Grange.[13] They also used a continuous single particle spectrum, but theirs is derived from a Green's function approach while ours is from a model space HF approach. Their single particle potential is generally complex, while ours is real. Nevertheless, the real parts of their single particle spectrum and our spectrum are numerically very close to each other for momentum $\lesssim 3$ fm^{-1}, with difference ≈ 10 MeV or less. (They used the real part of their single particle potential in their nuclear matter calculation.) Note that their spectrum is continuous for all momenta while ours has a small gap at k_M. It is rather satisfactory to note that the resulting BE/A and saturation k_F for their and our calculations are, respectively, (16.0±2 MeV, 1.62 fm^{-1}) and (15.5 MeV and 1.56 fm^{-1}). They are in remarkably good agreement. (Note that in addition to the above difference in the single particle spectrum, these two calculations also differ in methods of calculations. Their reaction matrix was obtained by solving differential equations in the coordinate space, while we have calculated our reaction matrix using the momentum space matrix inversion method.) The above confirms the general trend that nuclear matter calculations using a continuous single particle similar to the one derived in this work or that of Ref. 13 can increase the average nuclear matter binding energy by about 4 MeV, as compared with the conventional BHF results.

As discussed elsewhere,[5] the gain in BE/A from BHF to MBHF nuclear matter calculations is primarily due to the difference in the single particle spectrum used in these two calculations. The particle-hole gap in the single particle spectrum of MBHF is considerably smaller than that of BHF. Consequently, the energy denominators for low energy particle-hole excitations in nuclear matter are significantly reduced. This increases the contribution from these excitations to the nuclear matter binding energy, particularly for the $^3S_1$-$^3D_1$ channel (see Table II) where the NN tensor interaction is important.

The above gain in BE/A can also be explained from a different viewpoint. In BHF, the potential energy for a nucleon in the momentum region k_F to k_M is zero, while in MBHF it is generally attractive and has an average value of about -40 MeV. The probability of having a nucleon excited from $<k_F$ to the above momentum region is approximately given by the familiar wound integral whose value is found to be ~ 0.1. The potential energy for a nucleon below k_F in BHF and MBHF are approximately equal to each other. Hence the gain in BE/A from BHF to MBHF should be approximately $0.1\times(-40)=-4$ MeV. This estimate agrees well with the result shown in Fig. 3.

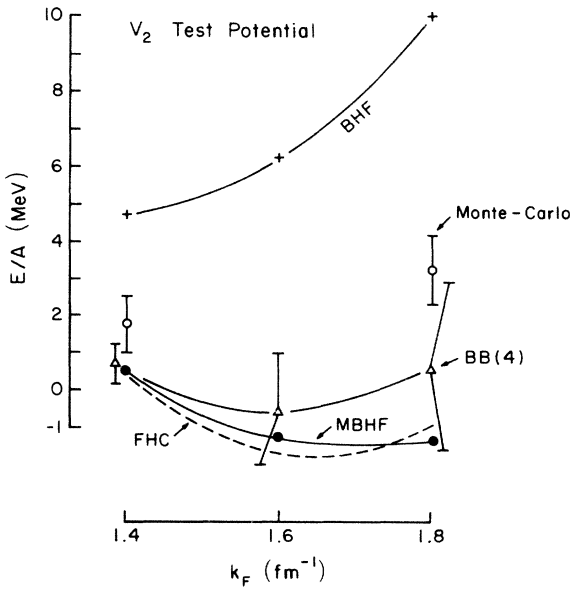

FIG. 4. Nuclear matter calculations using the V_2 test potential. Results of our calculations are denoted by BHF and MBHF. Those from the Green's function Monte-Carlo calculations (Ref. 17), the Fermi hypernetted chain calculations (Ref. 18), and Day's four-hole-line calculations (Ref. 19) are denoted by Monte-Carlo, FHC, and BB(4), respectively. Results for Monte Carlo and BB(4) are given with error estimates.

We have found that the contribution from the high-order partial waves ($l\gtrsim 4$) to the nuclear matter binding energy to be generally not important as indicated by Table II. This is consistent with the results of Sprung *et al.*[17] who estimated the contributions from high-order partial waves to nuclear matter binding energy directly from phase shifts, and the results of Grangé *et al.*[18] who investigated these contributions for nuclear matter calculations using continuous single particle spectra.

Although the calculated BE/A is in fairly good agreement with the empirical value, the calculated saturation density, however, is too high. We have investigated the effect of adding a weak density dependent central potential to the Paris NN potential. Although our investigation in this regard is rather preliminary, its results do indicate that we only need a rather *weak* (about 10% of the Paris central potential) additional density dependent central force to make the calculated BE/A and saturation k_F in simultaneous agreement with the empirical values.

To further present calculations, it seems to be of the highest priority to calculate some higher-order diagrams within the framework of MBHF. In MBHF, one essentially includes only the two-hole-line diagrams. Hence it is basically the same as BHF except for the use of the

MBHF continuous single particle spectrum as mentioned above. An important question to be answered is the following: Now that the MBHF BE/A is already in fairly good agreement with the empirical value, will this good agreement remain when one further includes some higher-order diagrams such as the ring diagrams within the model space? If it is so, then the net effect of all the higher-order diagrams must be small. It will be of much interest to find out if this turns out to be true. Ring diagram nuclear matter calculations using the Paris potential and the MBHF approach are now being carried out.[16]

To test the accuracy of the MBHF approach, we have carried out model nuclear matter calculations using the V_2 test potential. This potential is just the central part of the $^3S_1$ Reid NN potential, and for this potential highly accurate and elaborate nuclear matter calculations are available, namely the Monte-Carlo calculation,[19] the Fermi hypernetted chain calculation,[20] and Day's four-hole-line BHF calculation.[21] As shown in Fig. 4, our BHF results largely deviate from the results of these calculations. But our MBHF results agree with the latter two remarkably well. This is certainly an encouraging agreement.

Note added in proof. M. A. Matin and M. Dey [Phys. Rev. C **27**, 2356 (1983); **29**, 344 (1984)] have performed similar nuclear matter calculations and obtained BE/$A \approx 21$ MeV and a saturation point at $k_F \approx 1.6$ fm^{-1}.

ACKNOWLEDGMENTS

The authors are very grateful to Dr. B. D. Day for many stimulating discussions and advice, and for providing them with his unpublished results. Without them, this work would have not been possible. The authors are also very grateful to Prof. G. E. Brown for encouragement and many enlightening discussions, and to Dr. C. Hajduk for kindly providing them with his elaborate computer programs for computing the momentum-space matrix elements of the Paris potential. Finally Z.Y.M. and R.V.M. wish to thank Prof. G. E. Brown for his warm hospitality during their stay at Stony Brook. This work was supported in part by the U.S. Department of Energy Contract No. DE-AC02-76ER13001.

*Permanent address: Institute of Atomic Energy, P.O. Box 275(41), Beijing, The People's Republic of China.

†Permanent address: Division de Physique Theorique, Institut de Physique Nucleaire, 91406 Orsay, France.

[1]H. A. Bethe, Annu. Rev. Nucl. Sci. **21**, 93 (1971); D. W. L. Sprung, Adv. Nucl. Phys. **5**, 225 (1972); B. D. Day, Rev. Mod. Phys. **50**, 495 (1978).

[2]R. Jastrow, Phys. Rev. **98**, 1479 (1955); S. Fantoni and S. Rosati, Nuovo Cimento **A20**, 179 (1974).

[3]H. Kümmel, K. H. Lührmann, and J. G. Zabolitzky, Phys. Rep. **36C**, 1 (1978).

[4]Z. Y. Ma and T. T. S. Kuo, Phys. Lett. **B127**, 137 (1983).

[5]T. T. S. Kuo and Z. Y. Ma, in *Nucleon-Nucleon Interaction and Nuclear Many Body Problems,* edited by S. S. Wu and T. T. S. Kuo (World-Scientific, Singapore, 1984), p. 178.

[6]F. Coester, S. Cohen, B. Day, and C. M. Vincent, Phys. Rev. C **1**, 769 (1970).

[7]M. Lacombe, B. Loiseau, J. M. Richard, R. Vinh Mau, J. Coté, P. Pires, and R. de Tourreil, Phys. Rev. C **21**, 861 (1980).

[8]S. Barshay and G. E. Brown, Phys. Rev. Lett. **34**, 1106 (1975).

[9]A. D. Jackson, M. Rho, and E. Krotscheck, Nucl. Phys. **A407**, 495 (1983).

[10]J. P. Jeukenne, A. Lejeune, and C. Mahaux, Phys. Rep. **25**, 83 (1975).

[11]T. T. S. Kuo, S. Y. Lee, and K. F. Ratcliff, Nucl. Phys. **A176**, 65 (1971); T. T. S. Kuo, Annu. Rev. Nucl. Sci. **24**, 101 (1974); T. T. S. Kuo and E. M. Krenciglowa, Nucl. Phys. **A342**, 454 (1980).

[12]P. J. Ellis and E. Osnes, Rev. Mod. Phys. **49**, 777 (1977).

[13]A. Lejeune, M. Martzolff, and P. Grangé, *Lecture Notes in Physics* (Springer, Berlin, 1984), Vol. 198, p. 36.

[14]B. D. Day, private communication.

[15]B. D. Day, Phys. Rev. Lett. **47**, 226 (1981).

[16]H. Q. Song, S. D. Yang, and T. T. S. Kuo, private communication.

[17]D. W. L. Sprung, P. K. Banerjee, A. M. Jopko, and M. K. Scrivastava, Nucl. Phys. **A144**, 245 (1970).

[18]P. Grangé, A. Lejeune, and C. Mahaux, Nucl. Phys. **A319**, 50 (1979).

[19]D. Ceperley, G. V. Chester, and M. H. Kalos, Phys. Rev. B **16**, 3081 (1977).

[20]K. E. Schmidt and V. R. Pandharipande, Nucl. Phys. **A328**, 240 (1979).

[21]B. D. Day, Nucl. Phys. **A328**, 1 (1979).

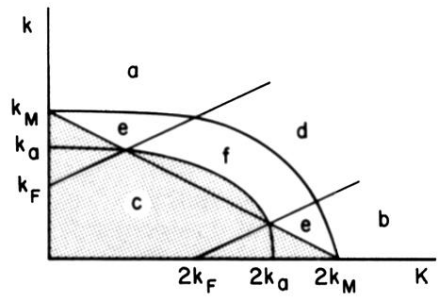

FIG. 1. Angle averaged projection operator $\overline{Q}(m,n)$ of Eq. (7). k_a^2 is $(k_F^2+k_M^2)/2$.